nature geoscience

REVIEW ARTICLE

https://doi.org/10.1038/s41561-018-0195-4

Lack of evidence for a substantial sea-level fluctuation within the Last Interglacial

Natasha L. M. Barlow[1*], Erin L. McClymont[2], Pippa L. Whitehouse[2], Chris R. Stokes[2], Stewart S. R. Jamieson[2], Sarah A. Woodroffe[2], Michael J. Bentley[2], S. Louise Callard[2], Colm Ó Cofaigh[2], David J. A. Evans[2], Jennifer R. Horrocks[2], Jerry M. Lloyd[2], Antony J. Long[2], Martin Margold[3], David H. Roberts[2] and Maria L. Sanchez-Montes[2]

During the Last Interglacial, global mean sea level reached approximately 6 to 9 m above the present level. This period of high sea level may have been punctuated by a fall of more than 4 m, but a cause for such a widespread sea-level fall has been elusive. Reconstructions of global mean sea level account for solid Earth processes and so the rapid growth and decay of ice sheets is the most obvious explanation for the sea-level fluctuation. Here, we synthesize published geomorphological and stratigraphic indicators from the Last Interglacial, and find no evidence for ice-sheet regrowth within the warm interglacial climate. We also identify uncertainties in the interpretation of local relative sea-level data that underpin the reconstructions of global mean sea level. Given this uncertainty, and taking into account our inability to identify any plausible processes that would cause global sea level to fall by 4 m during warm climate conditions, we question the occurrence of a rapid sea-level fluctuation within the Last Interglacial. We therefore recommend caution in interpreting the high rates of global mean sea-level rise in excess of 3 to 7 m per 1,000 years that have been proposed for the period following the Last Interglacial sea-level lowstand.

There is broad consensus that the highstand in global mean sea level (GMSL) during the Last Interglacial (LIG: Marine Isotope Stage (MIS) 5e; ~129–116 thousand years ago (ka)) was probably 6–9 m higher than present[1], implying a smaller than present global ice volume. Relative sea level (RSL), as recorded by proxy records, is locally variable[2] due to spatially non-uniform variations in the height of the geoid and the solid Earth and, as a result, local records of RSL do not reflect GMSL[3]. To better understand the structure of the GMSL highstand during the LIG, Kopp et al.[4] developed a global sea-level database that they statistically analysed to produce a posterior probability distribution of GMSL over the LIG (Fig. 1). That study, and further probabilistic analyses[5], highlight an interesting structure within the GMSL highstand: a 95% probability of a fluctuation (sea-level fall and rise) greater than 4 m (67% probability). Given that the Kopp analysis is corrected for local perturbations to the height of the land and sea surface, the primary mechanism invoked to explain the GMSL fall during the middle of the LIG is growth of one or more ice sheets[2]. However, sea-level data from the present interglacial provide no evidence for comparable (>4 m sea-level equivalent) ice-sheet regrowth[6]. Understanding the potential mechanism(s) for the LIG GMSL sea-level fall is important because the rates of GMSL rise that are inferred to have followed the lowstand are high[5] (likely, that is, 67% probability, between 3 and 7 m kyr^{-1}) and suggest a period of rapid ice-sheet collapse. Given the societal importance of the risks of future sea-level rise[7], it is vital to understand whether and how any lowstand occurred, because this constrains the subsequent high rates of GMSL rise in the LIG[4,8], which currently inform future climate adaptation assessments and strategies[7,9].

Understanding the nature of LIG sea-level change, and assessing the plausibility of the reconstructed GMSL lowstand, requires knowledge of four key elements, which we now consider in turn: (1) the solid Earth response to ice-sheet loading and unloading during and following the preceding glacial; (2) ice-sheet histories during the LIG; (3) thermosteric sea-level change; and (4) the quality of local RSL data which underpins the reconstruction.

Solid Earth processes

To reconstruct GMSL, it is important to identify the regional solid Earth processes that impact the elevation of former RSLs[10]. Kopp et al.[4,5] undertook this by running 250 alternative ice-sheet histories and randomly selected Earth viscosity profiles and using them in their Bayesian inversion to generate the GMSL curve shown in Fig. 1. In contrast, Düsterhus et al.[11] used a massive ensemble approach to analyse the same geological dataset, and performed 39,000 model runs, where the output of each run is a glacial isostatic adjustment (GIA)-based GMSL prediction associated with a specific ice-volume history and Earth model, which was subsequently evaluated by its fit to the RSL observations. Within the range of the most-probable runs, they found low variability within the interglacial and no notable GMSL lowstand. However, the variability and character of the ice-model history can have a large impact, and some of the lower-probability runs of Düsterhus et al.[11] show more sea-level variability within the interglacial.

The ice-history model inputs are important because RSL changes within an interglacial are greatly influenced by processes associated with the gradual relaxation of the solid Earth[10] following the collapse of the major ice sheets that defined the preceding glacial[3] (MIS 6). For example, the presence of large mid-latitude Northern Hemisphere ice sheets during MIS 6 will have led to the formation of extensive uplifted regions (peripheral bulges) surrounding the ice sheets, predominantly within ocean areas. Following the demise of the ice sheets, and if there was no further change in global ocean mass, gradual subsidence of the ocean-based peripheral bulges

[1]School of Earth and Environment, University of Leeds, Leeds, UK. [2]Department of Geography, Durham University, Lower Mountjoy, Durham, UK. [3]Department of Physical Geography, Stockholm University, Stockholm, Sweden. *e-mail: n.l.m.barlow@leeds.ac.uk

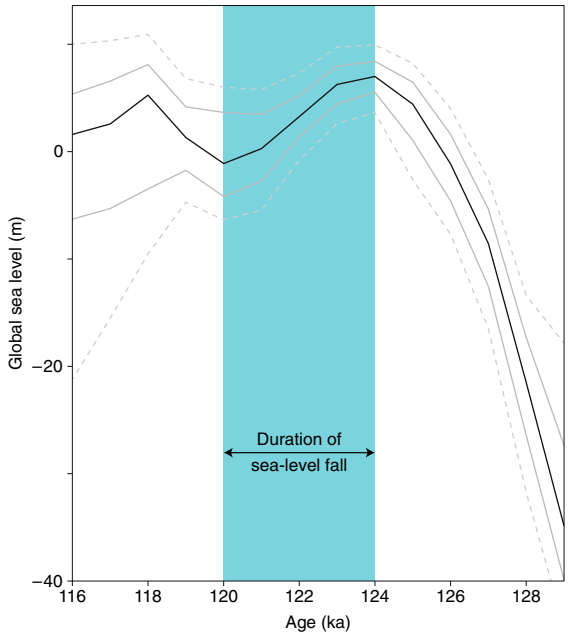

Fig. 1 | Probabilistic reconstruction of GMSL by Kopp et al.[4] during the LIG. The solid black line represents the median; solid grey lines the 16th and 84th percentiles; and dashed grey lines the 2.5th and 97.5th percentiles. The duration of sea-level fall depends on the uncertainties. It is very likely (95% probability) that the fastest rate of sea-level fall, prior to the final LIG sea-level decline, was 2.8 to 8.4 m kyr^{-1} (R. E. Kopp, personal communication). It is likely (67% probability) that the rates of GMSL rise that are inferred to have followed the lowstand are between 3 and 7 m kyr^{-1} (ref. [5]).

would result in far-field sea-level fall via a process known as ocean syphoning[12] (which partly explains a local sea-level fall recorded in Western Australia[13]). If this local sea-level fall driven by the solid Earth response was then overprinted by melting of the remaining ice sheets late in the interglacial, sufficient enough to cause a local sea-level rise, a RSL lowstand would be recorded in some locations[13].

Crucially, there is very little evidence to constrain the limits and volume of the MIS 6 ice sheets and, as such, the ice histories used by Kopp et al.[4,5] and Düsterhus et al.[11] are reliant on scaling oxygen isotope curves[14]. As the authors note, other effects, such as temperature, are present within these curves[15], and so they provide neither a direct analogue for total ice cover over time, nor, importantly, information on the spatial distribution of ice. Future research would therefore clearly benefit from improved constraints on the MIS 6 ice-sheet histories to constrain the magnitude and timing of the LIG GMSL highstand[16,17]. Recent work has also demonstrated that global-scale dynamic topography, driven by convective mantle flow, is relevant on the timescales of the LIG, and may impact upon the reconstructed peak GMSL by several metres[18]. However, due to the slow nature of mantle flow[19], this process cannot account for multimetre scale changes in sea level within the interglacial.

Kopp et al.[4] accounted for solid Earth processes when developing the GMSL reconstruction in Fig. 1, but doing this is challenging due to currently limited ice-sheet constraints, resulting in modelling uncertainties. As a response, we instead consider whether there is any direct evidence for ice-sheet regrowth during the LIG, which may drive a >4 m GMSL fall.

Possible mechanisms of ice-sheet (re)growth

For there to have been an increase in global ice volume of >4 m sea-level equivalent during the LIG (see Fig. 1), the Antarctic and/or Greenland ice sheets must have experienced positive mass balance and/or mid-latitude ice-sheet regrowth must have been initiated early in the LIG whilst temperatures were warmer than today[20] (Fig. 2 and Supplementary Information). Kopp et al.[5] suggested that it is very likely (within 95% confidence limits) that the fastest rate of sea-level fall, prior to the final LIG sea-level decline, was 2.8 to 8.4 m kyr^{-1} (R. E. Kopp, personal communication). We estimate that 1.15–3.45 million km^3 of net ice volume gain across Greenland and/or Antarctica over 1,000 years (equivalent to uniform thickening at a rate of 73–220 mm yr^{-1} across both ice sheets) would be necessary to explain this very likely range of sea-level fall rates (see Supplementary Information). To place these rates in context, the volume of the modern Greenland Ice Sheet (GrIS) is only 2.9 million km^3. Note that these estimates assume that ice discharge remained constant throughout the period of sea-level fall, and they therefore reflect minimum estimates for the rate at which ice sheets gained mass during the warmer climate and higher insolation conditions of the LIG (Fig. 2b).

Mechanisms of ice-sheet inception and growth are poorly constrained and largely theoretical, but there are five inter-related hypotheses that have been invoked (Fig. 3): (1) enhanced precipitation[21]; (2) ice saddle growth[22]; (3) instantaneous glacierization[23–25]; (4) marine ice transgression[26]; and (5) solid Earth feedbacks[27] — we now consider each of these in turn.

Early work on the North American ice-sheet complex[21] emphasized the importance of enhanced precipitation in the 'highland origin, windward growth' model (Fig. 3a). This suggests that ice sheets originate as highland snow-fields that grow fastest towards the prevailing wind direction. The saddle formation hypothesis (Fig. 3b) emphasizes the role of topography[22] such that where two high-elevation ice masses coalesce, the formation of a saddle is likely to lead to rapid growth. This involves positive feedbacks between albedo and ice-sheet elevation/precipitation, and requires the initial development of independent regional ice centres. The instantaneous glacierization mechanism (Fig. 3c) emphasizes the importance of upland plateaus that are close to the threshold of glaciation[23–25]. Climatic cooling could lower the regional snowline, such that plateau snow-fields rapidly increase in number and size, and the expanding snow-fields then thicken to become ice sheets[26]. In contrast, the marine ice transgression hypothesis[26] (Fig. 3d) emphasizes the importance of sea-ice formation across shallow marine basins. Here, climatic cooling leads to sea-ice formation, which in turn lowers the regional albedo. This process could theoretically allow the sea ice to thicken to form ice shelves (*sensu lato*) that become grounded in shallow water, creating marine ice domes that expand to form an ice sheet[26]. Finally, solid Earth rebound in response to ice loss (Fig. 3e), particularly in regions underlain by low upper mantle viscosity (for example, West Antarctica[28]), could lead to grounding-line advance. The formation of ice rises[29] during this process could also help to stabilize the ice sheet due to their buttressing effect[30]. Such solid Earth feedbacks have recently been invoked to explain grounding line re-advance in West Antarctica during the Holocene[31], but the magnitude of the associated sea-level fall is predicted to have been an order of magnitude smaller than suggested by Kopp et al.[4,5] for the LIG. In considering whether one or more of these mechanisms could be important for ice-sheet regrowth during the LIG, it is important to note that these mechanisms are not mutually exclusive, and that their relative importance may vary between ice masses and/or through time. Furthermore, these are hypothesized mechanisms and the rates and magnitudes of change, under differing climate conditions, are largely unknown. Given these potential mechanisms, we evaluate the geomorphological, glaciological and modelling evidence for ice-sheet regrowth during the LIG.

Evidence for LIG ice-sheet (re)growth

Compared to the glacial maxima of MIS 6 and 2, the GrIS was much reduced and largely terrestrial during the LIG[32], with

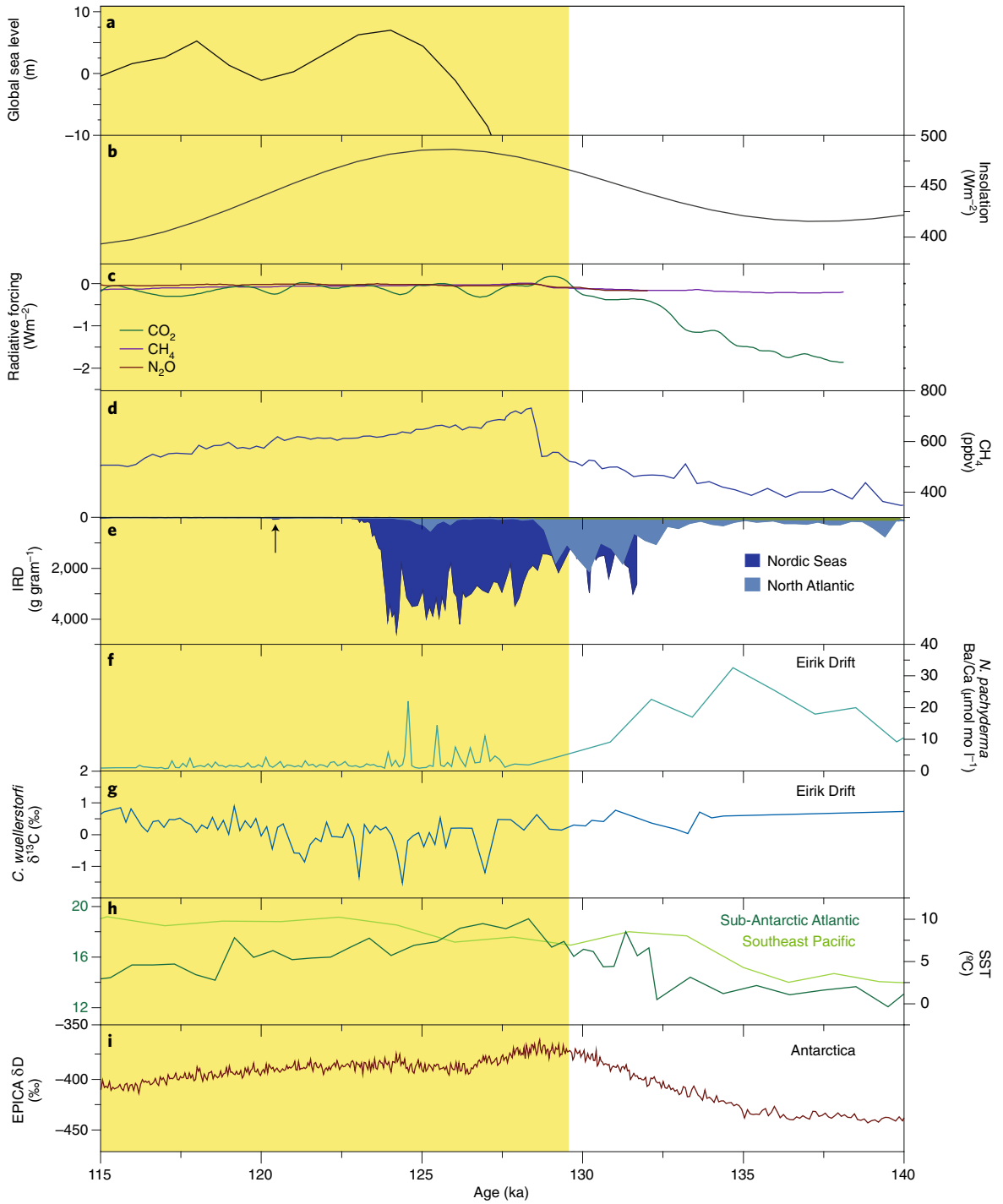

Fig. 2 | Selected records indicating climate changes and/or ice-sheet changes during the LIG. MIS 5e is shaded yellow. **a**, Global sea-level reconstruction (median value)[4]. **b**, July insolation at 65° N (ref. [100]). **c**, Radiative forcing variations driven by the major greenhouse gases[101]. **d**, Antarctic methane concentrations[102], which reflect Greenland's temperature[62]. **e**, IRD from the Nordic seas[82] and North Atlantic[103]. Bauch et al.[82] highlight a small increase in IRD at 120–121 ka (marked by the arrow). **f**, Planktonic foraminifera Ba/Ca ratios from Eirik Drift, a proxy for Greenland ice-sheet melt[44]. **g**, Eirik Drift benthic δ^{13}C (3,442 m), a proxy for Atlantic meridional overturning circulation strength[44]. **h**, Southeast Pacific SSTs, offshore of Patagonia[104], and sub-Antarctic Atlantic SSTs[105]. **i**, European Project for Ice Coring in Antarctica (EPICA) δD as a proxy for Antarctic air temperature[106]. *N. pachyderma*, *Neogloboquadrina pachyderma*; *C. wuellerstorfi*, *Cibicidoides wuellerstorfi*.

marine-terminating glaciers probably only present in the east[33]. Model simulations of the LIG GrIS[33–36] indicate that increased air temperatures and higher insolation led to a negative surface mass balance across much of the ice sheet[37]. Radar data suggest that ice was present in central and northern Greenland, but identifying the full extent of LIG ice is methodologically challenging[38]. Offshore records suggest a restricted LIG GrIS based on pollen concentrations that are five times higher than in the Holocene[39], while geochemical proxies indicate sustained ice surface melt[40–42]. Ice-rafted debris (IRD) with a southern Greenland provenance[43] suggests

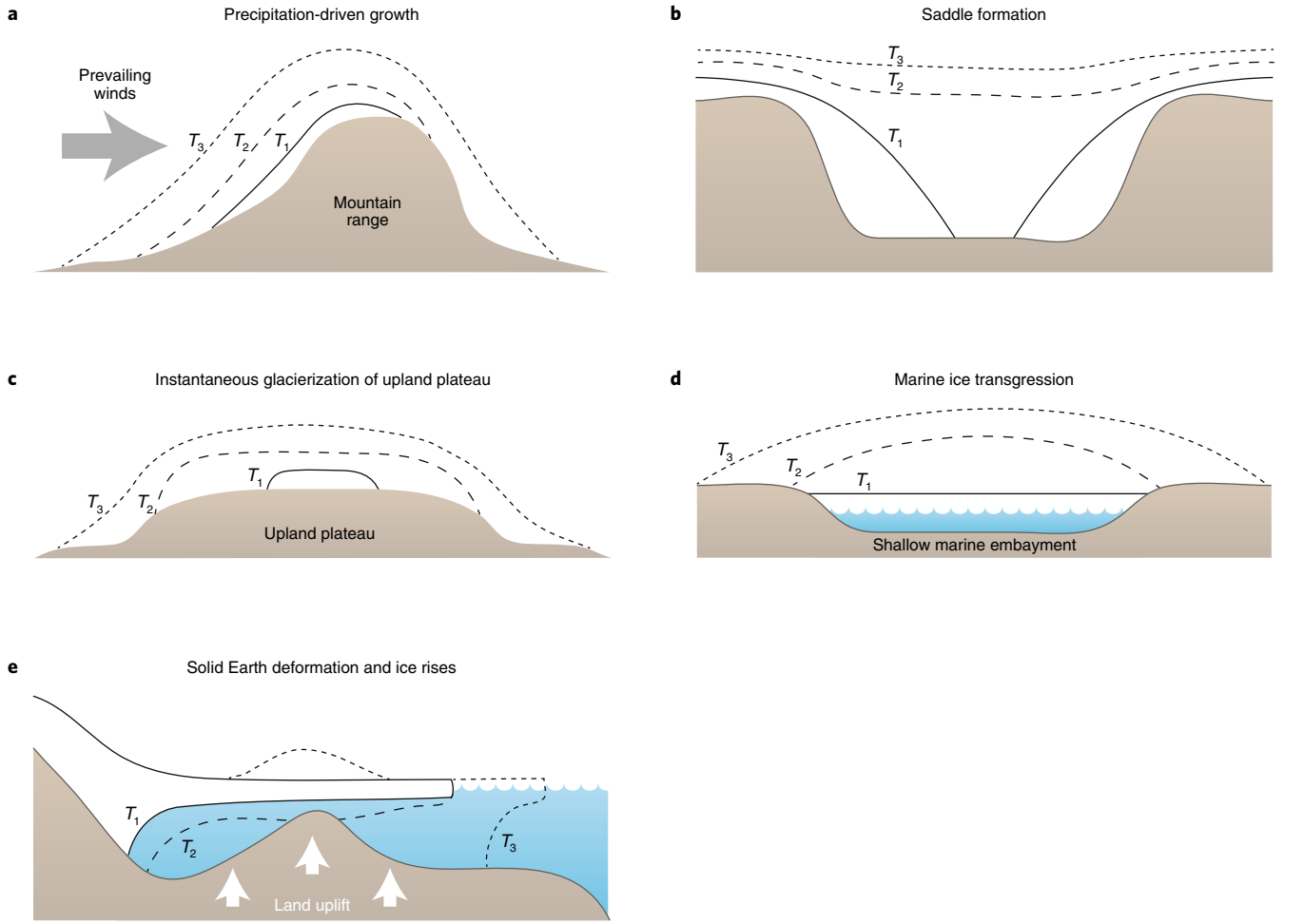

Fig. 3 | Theoretical mechanisms of ice-sheet growth and inception. Three successive time steps (T_1, T_2, T_3) are shown.

centennial-scale oscillations and glacial meltwater inputs until 124 ka (ref. [44]) (Fig. 2f). The low input of IRD is consistent with a smaller ice sheet compared to glacial maxima, but the presence of IRD indicates that some outlet glaciers reached the ocean. However, none of the Greenland records or models point unequivocally to periods of pronounced ice regrowth during the LIG.

Direct evidence for the extent and thickness of the Antarctic Ice Sheet during the LIG is limited[45–47]. Marine sediment records in the Ross and Weddell seas detail evidence for collapse (and regrowth) of the West Antarctic Ice Sheet (WAIS) during the mid and late Pleistocene, but dating precision is insufficient to confidently attribute this to the LIG[48]. The ANDRILL record in the Ross Sea indicates that multiple cyclic fluctuations between subglacial, ice-proximal, ice-distal and open marine conditions occurred during the Pleistocene[49] but it does not appear to indicate any evidence of ice-sheet regrowth during the LIG, instead showing a transition from proximal grounding-line sedimentation to distal and perhaps open marine conditions. Records from the Amundsen and Bellingshausen seas show no evidence for interglacial WAIS collapse (nor expansion) since at least MIS 13 (refs [50–52]). Onshore evidence points to only minor changes in ice surface elevation in the central parts of the WAIS during the LIG[46,53]. Thus, there is little direct evidence for significant changes in WAIS extent during the LIG.

Similar to the WAIS, direct evidence for any changes to the East Antarctic Ice Sheet (EAIS) extent during the LIG are not well constrained. In the McMurdo Dry Valleys, Taylor Glacier expanded slightly, depositing the Bonney drift during the LIG[54] when the Taylor Dome ice core also shows evidence for regional thickening of up to ~70 mm yr^{-1} (ref. [55]). In the Larsemann Hills, Princess Elizabeth Land, lake cores reveal warm biota and an active hydrological system, implying ice-free conditions for ~10,000 years prior to an abrupt transition to glacial conditions at around 120 ka (ref. [56]). Extrapolating these limited local records to understand the behaviour, and possible LIG regrowth, of the entire EAIS is not possible. Some changes in isotopic-derived temperature records within EAIS ice cores could reflect ice-elevation changes associated with ice-sheet mass balance[57]. However, existing ice cores are not optimally located to unambiguously identify elevation changes associated with changes in either the WAIS or the Aurora, Wilkes and Recovery basins of the EAIS, where any changes might first be expected[57–60].

Two recent Antarctic modelling studies simulated significant interglacial ice volume change. One includes rapid ice-shelf loss and subsequent retreat via an ice-cliff-fracturing mechanism coupled with atmospheric warming[60]. The outputs are generally consistent with the estimate by Kopp et al.[4] for the Antarctic contribution to GMSL during the LIG, but produce no notable mid-LIG RSL lowstand. The second modelling study proposes that a combination of marine ice-sheet instability, warm subsurface ocean temperatures and variations in surface accumulation could result in a double-peaked contribution of WAIS melt to LIG sea level[61]. By invoking a potential subsurface ocean-cooling episode, flanked by increases in the surface mass balance, the model outputs suggest a potential

recovery in ice volume between the two stages of collapse. However, this requires a +2 to +3 °C Southern Ocean temperature anomaly, which is greater than the +1.2 °C recorded in the palaeo data[62], but perhaps not implausible given the average 2.6 °C 2σ uncertainty stated for those proxy records[62].

The LIG was warmer than present, and models that explore Antarctic ice-sheet response to future warming indicate that enhanced precipitation, particularly in the EAIS, would increase surface mass balance[63] but suggest that this would be counteracted by enhanced surface melt near the coast[64], resulting in limited net change in ice-sheet volume. Thus, although there is some evidence for a very minor advance of marginal areas of the EAIS during the LIG, there is no unequivocal evidence of significant regrowth. Only by invoking ocean warming >2 °C is it possible to simulate a double-peak in sea level due to changes in Antarctic ice volume[61].

Beyond the polar regions, the general consensus is that there was no Laurentide Ice Sheet (LIS) during the LIG[65], with most evidence pointing towards inception after 120 ka (ref. [66]), that is, after the period of proposed GMSL fall (Fig. 1). An abrupt drainage event recorded in a proximal marine core in the Labrador Sea is attributed to former glacial Lake Agassiz in the Hudson Bay region at approximately 124.5 ka (ref. [67]), which may provide indirect evidence of some Laurentide ice early in the LIG, but not for regrowth within the LIG. The primary evidence for a general absence of LIG Laurentide ice comes from dated organic-rich sediments in the Hudson Bay Lowlands[68], which could not have formed under ice cover. Whilst different dating techniques have provided slightly different ages for these sediments, recent work[68] gives clusters of ages that suggest the area was ice free during the middle of the LIG.

In Eurasia, it is generally accepted that there was an extensive MIS 6 ice sheet, but there is only limited and imprecise dating of the ice retreat prior to the LIG. Along the northern margin of Eurasia there is sedimentary evidence for a major marine transgression during the LIG and a complete disappearance of the Eurasian Ice Sheet (EIS)[69,70]. Warm conditions and the absence of glaciation are also recorded by intermorainic organic deposits on the Scandinavian Peninsula: the main inception area of the Fennoscandian sector of the EIS[71,72]. As with the LIS, rapid EIS growth is documented following the MIS 5e–d transition[73,74], but the EIS is an unlikely candidate for driving sea-level fluctuations within the LIG.

Evidence relating to smaller ice masses such as plateau icefields and valley glaciers in Alaska, Patagonia, Iceland, the European Alps, Siberia, the Himalaya and Southern Alps is sparse, with no direct evidence for LIG ice in these regions[75–78]. Moreover, although there is potential for LIG ice to have been present in mountainous regions covered by ice caps and glaciers today, their small net volume[7] (total modern mean sea-level equivalent of 0.4 m) makes it unlikely that these small ice masses could drive multimetre GMSL fluctuations during peak LIG warmth.

In summary, there is no empirical evidence to support the hypothesis of ice-sheet regrowth of sufficient magnitude to explain the putative GMSL fluctuation. The only potential sites where ice-sheet regrowth of a significant volume could have theoretically occurred during the LIG are Antarctica and Greenland, as other ice masses were either absent or too small to account for a multimetre sea-level fall. In addition, the sea-level fluctuation cannot be explained by an out-of-phase melting of Greenland and Antarctica during the LIG, as there must be a period of net ice increase to cause a fall in GMSL. The absence of evidence of ice regrowth may also reflect the difficulty of constraining pre-LGM ice-sheet dynamics where subsequent glacial advances may have overprinted or erased evidence. However, the lack of evidence for regrowth is largely consistent with modelling studies (perhaps with the exception of Sutter et al.[61]), which are unable to model ice-sheet-driven sea-level variations on millennial timescales during the LIG[79].

The role of thermal expansion

The absence of geomorphological or stratigraphical evidence for ice-sheet regrowth during the LIG leads us to consider the only other mechanism that might explain the GMSL fall as presented in Fig. 1: thermosteric sea-level change. Kopp et al.[4] estimate a thermosteric component in their modelling, which varies with global ice volume (–1.6 ± 0.6 m per 100 m equivalent sea-level ice-sheet growth). Based on a compilation of LIG sea surface temperature (SST) data and a coupled atmosphere–ocean climate model, McKay et al.[80] suggest that it is unlikely that thermosteric sea-level rise exceeded 0.4 ± 0.3 m during the LIG. On millennial timescales, the equilibrium response of ocean thermal expansion to warming has been estimated as 0.2 to 0.6 m per °C (ref. [81]). If simply inverted for cooling and the consequent thermal contraction (without including potential changes in ocean stratification), a 4 m sea-level fall (Fig. 1) would require a ~6–20 °C global temperature drop during the LIG, which is clearly not evident[62]. Regionally cooler SSTs, such as in the Nordic seas[82], may have driven a small, localized thermosteric contraction, but not one that resulted in a multimetre global sea-level fall.

LIG relative sea-level data

The absence of direct evidence for ice-sheet regrowth or thermosteric cooling sufficient to drive a >4 m sea-level fall during the LIG leads us to review the data, which underpins the GMSL curve in Fig. 1. Reconstructions of GMSL must be supported by local RSL data which includes a location, age, elevation (both the measured elevation of the sample and the modern relationship to the tide level at which such an indicator would form today) and, ideally, a summary of whether the indicator describes an increase or decrease in marine influence[83,84]. The Kopp et al.[4] dataset comprises 108 RSL observations from 47 sites. The highly fluctuating Red Sea record[8] (based on stable oxygen isotopes of planktonic foraminifera) provides 29 of the sea-level observations in the dataset and plays an important role in anchoring the timescale (although the timing of the highstand has since been revised by 6,300 years[85]). Kopp et al.[5] show that their reconstructed GMSL fall is not precluded by the inclusion of the Red Sea data. Outside of the Red Sea basin, the most widespread LIG sea-level archives (both within the Kopp et al. database and in records published since) are preserved in low-latitude regions. They are therefore typically based on fossil corals and reef terraces[10,86,87], some of which provide potential evidence for one or more local RSL falls[86,88,89]. A recent comprehensive analysis of modern coral distributions[90] has shown that there is no direct relationship between coral growth and water depth per se, and that coral-depth distributions are clearly variable. This suggests notable uncertainties in the elevation of former sea levels reconstructed by some records[86,88,89,91]. Reworked corals are also common in Barbados, which can result in erroneous interpretations of past sea level[92]. Furthermore, using coral archives as LIG sea-level records is complicated by uncertainty surrounding the use of open- versus closed-system uranium–thorium (U–Th) ages[93], with a compilation of closed-system U–Th ages from corals in West Australia, Bahamas, Bermuda and Yucatan providing no evidence for a local sea-level fall within the interglacial[10].

These issues raise an important question: after accounting for solid Earth processes, is there any clear empirical evidence for a global mean sea-level fall of >4 m during the LIG? In the Seychelles — a site predicted to approximately record GMSL[94] — there appears to be a regionally consistent interruption to LIG reef growth, potentially indicative of a stable or briefly falling RSL, or alternatively caused by changes in local accommodation space or storm bleaching[87,95]. A mid-interglacial falling RSL is suggested by a survey of palaeo-shorelines in Western Australia, but the authors explain this by regional solid Earth processes[13]. In Southern Australia, sedimentary evidence points to a single phase of sea-level rise[96], while on the Yucatán peninsula, Mexico, LIG RSL was

stable until a rapid late-interglacial sea-level rise[97]. Such records could be produced if falling GMSL was matched by local land subsidence. However, given that GMSL fall is estimated to be ~3–8 m in 1,000 years, subsidence would need to be very rapid to prevent a hiatus being recorded in the stratigraphy at these sites. A Mediterranean facies succession, previously interpreted to record a double LIG highstand[88], has recently been reinterpreted as providing no evidence of a LIG RSL fall, instead recording highstands from two separate interstadials[98]. In temperate-latitude locations, there is no evidence for local LIG RSL oscillations[2,99]. Without unequivocal empirical evidence for locally falling sea level[96,98], and considering the uncertainties in coral-growth distributions[90], the local RSL data provide limited support for >4 m fluctuations in GMSL during the middle of the LIG.

Conclusion

In conclusion, reconstructions of GMSL during the LIG[4,5] have raised the intriguing possibility that fluctuations in ice-sheet volume occurred within the interglacial, that is, ice sheets regrew and then decayed. We have considered several possible driving mechanisms, acting alone or in combination, for multimetre changes in GMSL during the LIG. We find that the current understanding of ice-sheet histories during MIS 6 is not adequate enough to rule out the possibility that limitations in the modelling of the solid Earth response could be contributing to the appearance of a GMSL fall during the LIG[3,11]. However, if the GMSL fall was driven by changes in ice-sheet mass balance, it would require 1.15–3.45 million km^3 of ice to form in less than 1,000 years; we found little geomorphological or sedimentary evidence for such substantial ice-sheet regrowth during the LIG. It is also clear that large uncertainties associated with the interpretation of some local RSL data that underpin the reconstructed GMSL curve remain. Taken together, our analysis leads us to question the occurrence of a rapid GMSL fall within the LIG, which also raises important questions about the very high reconstructed rates of GMSL rise following the lowstand; reported to be approximately 3 to 7 m kyr^{-1} (ref. [5]).

We conclude that it is critical that future reconstructions of GMSL during the LIG include a range of realistic ice-sheet scenarios from the preceding glacial (MIS 6); take into account the impact of dynamic topography on the reconstructed elevations of former RSLs; and assemble a geographically and temporally widespread dataset of local RSL, with careful interpretation of fossil sea-level indicators with respect to tidal datums and accurate chronologies. Until these issues are better resolved, we would urge caution in using rates of GMSL rise from the LIG to project future sea-level changes.

Received: 10 March 2017; Accepted: 2 July 2018;
Published online: 6 August 2018

References

1. Dutton, A. et al. Sea-level rise due to polar ice-sheet mass loss during past warm periods. *Science* **349**, aaa4019 (2015).
2. Long, A. J. et al. Near-field sea-level variability in northwest Europe and ice sheet stability during the last interglacial. *Quat. Sci. Rev.* **126**, 26–40 (2015).
3. Lambeck, K., Purcell, A. & Dutton, A. The anatomy of interglacial sea levels: the relationship between sea levels and ice volumes during the Last Interglacial. *Earth Planet. Sci. Lett.* **315**, 4–11 (2012).
4. Kopp, R. E., Simons, F. J., Mitrovica, J. X., Maloof, A. C. & Oppenheimer, M. Probabilistic assessment of sea level during the last interglacial stage. *Nature* **462**, 863–867 (2009).
5. Kopp, R. E., Simons, F. J., Mitrovica, J. X., Maloof, A. C. & Oppenheimer, M. A probabilistic assessment of sea level variations within the last interglacial stage. *Geophys. J. Int.* **193**, 711–716 (2013).
6. Lambeck, K., Rouby, H., Purcell, A., Sun, Y. & Sambridge, M. Sea level and global ice volumes from the Last Glacial Maximum to the Holocene. *Proc. Natl. Acad. Sci. USA* **111**, 15296–15303 (2014).
7. IPCC *Climate Change 2013: The Physical Science Basis* (eds Stocker, T. F. et al.) (Cambridge Univ. Press, Cambridge, 2013).
8. Rohlin, E. J. et al. High rates of sea-level rise during the last interglacial period. *Nat. Geosci.* **1**, 38–42 (2008).
9. Lowe, J. A. et al. *UK Climate Projections Science Report: Marine and Coastal Projections* (UK Climate Projections, 2009).
10. Dutton, A. & Lambeck, K. Ice volume and sea level during the Last Interglacial. *Science* **337**, 216–219 (2012).
11. Düsterhus, A., Tamisiea, M. E. & Jevrejeva, S. Estimating the sea level highstand during the Last Interglacial: a probabilistic massive ensemble approach. *Geophys. J. Int.* **206**, 900–920 (2016).
12. Mitrovica, J. X. & Peltier, W. R. On postglacial geoid subsidence over the equatorial oceans. *J. Geophys. Res.* **96**, 20053–20071 (1991).
13. O'Leary, M. J. et al. Ice sheet collapse following a prolonged period of stable sea level during the last interglacial. *Nat. Geosci.* **6**, 796–800 (2013).
14. Lisiecki, L. E. & Raymo, M. E. A Pliocene-Pleistocene stack of 57 globally distributed benthic $\delta^{18}O$ records. *Paleoceanography* **20**, PA1003 (2005).
15. Shackleton, N. J. Oxygen isotopes, ice volume and sea level. *Quat. Sci. Rev.* **6**, 183–190 (1987).
16. Dendy, S., Austermann, J., Creveling, J. R. & Mitrovica, J. X. Sensitivity of Last Interglacial sea-level high stands to ice sheet configuration during Marine Isotope Stage 6. *Quat. Sci. Rev.* **171**, 234–244 (2017).
17. Rohling, E. J. Differences between the last two glacial maxima and implications for ice-sheet, $\delta^{18}O$, and sea-level reconstructions. *Quat. Sci. Rev.* **176**, 1–28 (2017).
18. Austermann, J., Mitrovica, J. X., Huybers, P. & Rovere, A. Detection of a dynamic topography signal in last interglacial sea-level records. *Sci. Adv.* **3**, e1700457.
19. Moucha, R. et al. Dynamic topography and long-term sea-level variations: there is no such thing as a stable continental platform. *Earth Planet. Sci. Lett.* **271**, 101–108 (2008).
20. Past Interglacials Working Group of PAGES. Interglacials of the last 800,000 years. *Rev. Geophys.* **54**, 162–219 (2016).
21. Flint, R. F. Growth of North American ice sheet during the Wisconsin age. *Geol. Soc. Am. Bull.* **54**, 325–362 (1943).
22. Payne, A. & Sugden, D. Topography and ice sheet growth. *Earth Surf. Process. Landf.* **15**, 625–639 (1990).
23. Williams, L. D. Ice-sheet initiation and climatic influences of expanded snow cover in Arctic Canada. *Quat. Res.* **10**, 141–149 (1978).
24. Williams, L. D. An energy balance model of potential glacierization of northern Canada. *Arct. Antarct. Alp. Res.* **11**, 443–456 (1979).
25. Bromwich, D. H., Toracinta, E. R. & Wang, S.-H. Meteorological perspective on the initiation of the Laurentide Ice Sheet. *Quat. Int.* **95**, 113–124 (2002).
26. Hughes, T. J. The marine ice transgression hypothesis. *Geografiska Annaler A* **69**, 237–250 (1987).
27. Gomez, N., Mitrovica, J. X., Huybers, P. & Clark, P. U. Sea level as a stabilizing factor for marine-ice-sheet grounding lines. *Nat. Geosci.* **3**, 850–853 (2010).
28. van der Wal, W., Whitehouse, P. L. & Schrama, E. J. Effect of GIA models with 3D composite mantle viscosity on GRACE mass balance estimates for Antarctica. *Earth Planet. Sci. Lett.* **414**, 134–143 (2015).
29. Matsuoka, K. et al. Antarctic ice rises and rumples: their properties and significance for ice-sheet dynamics and evolution. *Earth Sci. Rev.* **150**, 724–745 (2015).
30. Favier, L. & Pattyn, F. Antarctic ice rise formation, evolution, and stability. *Geophys. Res. Lett.* **42**, 4456–4463 (2015).
31. Kingslake, J. et al. Extensive retreat and re-advance of the West Antarctic Ice Sheet during the Holocene. *Nature* **558**, 430–434 (2018).
32. Funder, S., Kjeldsen, K. K., Kjær, K. H. & Cofaigh, C. The Greenland Ice Sheet during the past 300,000 years: a review. *Dev. Quat. Sci.* **15**, 699–713 (2011).
33. Calov, R., Robinson, A., Perrette, M. & Ganopolski, A. Simulating the Greenland ice sheet under present-day and palaeo constraints including a new discharge parameterization. *Cryosphere* **9**, 179–196 (2015).
34. Robinson, A., Calov, R. & Ganopolski, A. Greenland ice sheet model parameters constrained using simulations of the Eemian Interglacial. *Clim. Past.* **7**, 381–396 (2011).
35. Otto-Bliesner, B. L., Marshall, S. J., Overpeck, J. T., Miller, G. H. & Hu, A. Simulating Arctic climate warmth and icefield retreat in the last interglaciation. *Science* **311**, 1751–1753 (2006).
36. Helsen, M. et al. Coupled regional climate-ice-sheet simulation shows limited Greenland ice loss during the Eemian. *Clim. Past.* **9**, 1773–1788 (2013).
37. van de Berg, W. J., van den Broeke, M., Ettema, J., van Meijgaard, E. & Kaspar, F. Significant contribution of insolation to Eemian melting of the Greenland ice sheet. *Nat. Geosci.* **4**, 679–683 (2011).
38. MacGregor, J. A. et al. Radiostratigraphy and age structure of the Greenland Ice Sheet. *J. Geophys. Res.* **120**, 212–241 (2015).
39. de Vernal, A. & Hillaire-Marcel, C. Natural variability of Greenland climate, vegetation, and ice volume during the past million years. *Science* **320**, 1622–1625 (2008).
40. Carlson, A. E., Stoner, J. S., Donnelly, J. P. & Hillaire-Marcel, C. Response of the southern Greenland Ice Sheet during the last two deglaciations. *Geology* **36**, 359–362 (2008).

41. Carlson, A. E. & Winsor, K. Northern Hemisphere ice-sheet responses to past climate warming. *Nat. Geosci.* **5**, 607–613 (2012).
42. Colvill, E. J. et al. Sr-Nd-Pb isotope evidence for ice-sheet presence on southern Greenland during the Last Interglacial. *Science* **333**, 620–623 (2011).
43. Reye, A. V. et al. South Greenland ice-sheet collapse during Marine Isotope Stage 11. *Nature* **510**, 525–528 (2014).
44. Galaasen, E. V. et al. Rapid reductions in North Atlantic Deep Water during the peak of the last interglacial period. *Science* **343**, 1129–1132 (2014).
45. Steig, E. J. et al. Influence of West Antarctic Ice Sheet collapse on Antarctic surface climate. *Geophys. Res. Lett.* **42**, 4862–4868 (2015).
46. Hein, A. S. Evidence for the stability of the West Antarctic Ice Sheet divide for 1.4 million years. *Nat. Commun.* **7**, 10325 (2016).
47. EPICA community members. Eight glacial cycles from an Antarctic ice core. *Nature* **429**, 623–628 (2004).
48. Vaughan, D. G., Barnes, D. K., Fretwell, P. T. & Bingham, R. G. Potential seaways across west Antarctica. *Geochem. Geophys. Geosyst.* **12**, Q10004 (2011).
49. McKay, R. et al. Pleistocene variability of Antarctic ice sheet extent in the Ross embayment. *Quat. Sci. Rev.* **34**, 93–112 (2012).
50. Cofaigh, C. O., Dowdeswell, J. A. & Pudsey, C. J. Late Quaternary iceberg rafting along the Antarctic Peninsula continental rise and in the Weddell and Scotia seas. *Quat. Res.* **56**, 308–321 (2001).
51. Hillenbrand, C.-D., Fütterer, D. K., Grobe, H. & Frederichs, T. No evidence for a Pleistocene collapse of the West Antarctic Ice Sheet from continental margin sediments recovered in the Amundsen Sea. *Geo. Mar. Lett.* **22**, 51–59 (2002).
52. Hillenbrand, C. D., Kuhn, G. & Frederichs, T. Record of a Mid-Pleistocene depositional anomaly in West Antarctic continental margin sediments: an indicator for ice-sheet collapse? *Quat. Sci. Rev.* **28**, 1147–1159 (2009).
53. Ackert, R. P. Jr et al. West Antarctic Ice Sheet elevations in the Ohio Range: geologic constraints and ice sheet modeling prior to the last highstand. *Earth Planet. Sci. Lett.* **307**, 83–93 (2011).
54. Higgins, S., Denton, G. H. & Hendy, C. H. Glacial geomorphology of Bonney drift, Taylor Valley, Antarctica. *Geografiska Annaler A* **82**, 365–389 (2000).
55. Steig, E. J. et al. Wisconsinan and Holocene climate history from an ice core at Taylor Dome, Western Ross Embayment, Antarctica. *Geogr. Ann.: Ser. A. Phys. Geogr.* **82**, 213–235 (2000).
56. Hodgso, D. A. et al. Interglacial environments of coastal east Antarctica: comparison of MIS 1 (Holocene) and MIS 5e (Last Interglacial) lake-sediment records. *Quat. Sci. Rev.* **25**, 179–197 (2006).
57. Bradley, S., Siddall, M., Milne, G., Masson-Delmotte, V. & Wolff, E. Where might we find evidence of a Last Interglacial West Antarctic Ice Sheet collapse in Antarctic ice core records? *Glob. Planet. Change* **88**, 64–75 (2012).
58. Mengel, M. & Levermann, A. Ice plug prevents irreversible discharge from East Antarctica. *Nat. Clim. Change* **4**, 451–455 (2014).
59. Pollard, D., DeConto, R. M. & Alley, R. B. Potential Antarctic ice sheet retreat driven by hydrofracturing and ice cliff failure. *Earth Planet. Sci. Lett.* **412**, 112–121 (2015).
60. DeConto, R. M. & Pollard, D. Contribution of Antarctica to past and future sea-level rise. *Nature* **531**, 591–597 (2016).
61. Sutter, J., Gierz, P., Grosfeld, K., Thoma, M. & Lohmann, G. Ocean temperature thresholds for Last Interglacial West Antarctic Ice Sheet collapse. *Geophys. Res. Lett.* **43**, 2675–2682 (2016).
62. Capron, E. et al. Temporal and spatial structure of multi-millennial temperature changes at high latitudes during the Last Interglacial. *Quat. Sci. Rev.* **103**, 116–133 (2014).
63. Ligtenberg, S. R. M., van de Berg, W. J., van den Broeke, M. R., Rae, J. G. L. & van Meijgaard, E. Future surface mass balance of the Antarctic ice sheet and its influence on sea level change, simulated by a regional atmospheric climate model. *Clim. Dynam.* **41**, 867–884 (2013).
64. Lenaerts, J. T. M., Vizcaino, M., Fyke, J., van Kampenhout, L. & van den Broeke, M. R. Present-day and future Antarctic ice sheet climate and surface mass balance in the community Earth system model. *Clim. Dynam.* **47**, 1367–1381 (2016).
65. Kleman, J. et al. North American Ice Sheet build-up during the last glacial cycle, 115–21 kyr. *Quat. Sci. Rev.* **29**, 2036–2051 (2010).
66. Stokes, C. R., Tarasov, L. & Dyke, A. S. Dynamics of the North American Ice Sheet Complex during its inception and build-up to the Last Glacial Maximum. *Quat. Sci. Rev.* **50**, 86–104 (2012).
67. Nicholl, J. A. L. A Laurentide outburst flooding event during the last interglacial period. *Nat. Geosci.* **5**, 901–904 (2012).
68. Allard, G. et al. Constraining the age of the last interglacial–glacial transition in the Hudson Bay lowlands (Canada) using U–Th dating of buried wood. *Quat. Geochron.* **7**, 37–47 (2012).
69. Spielhagen, R. F. et al. Arctic Ocean deep-sea record of northern Eurasian ice sheet history. *Quat. Sci. Rev.* **23**, 1455–1483 (2004).
70. Svendsen, J. I. et al. Late Quaternary ice sheet history of northern Eurasia. *Quat. Sci. Rev.* **23**, 1229–1271 (2004).
71. Lundqvist, J. Glacial history of Sweden. *Dev. Quat. Sci.* **2**, 401–412 (2004).
72. Mangerud, J. Ice sheet limits in Norway and on the Norwegian continental shelf. *Dev. Quat. Sci.* **2**, 271–294 (2004).
73. Möller, P., Alexanderson, H., Funder, S. & Hjort, C. The Taimyr Peninsula and the Severnaya Zemlya archipelago, Arctic Russia: a synthesis of glacial history and palaeo-environmental change during the Last Glacial cycle (MIS 5e–2). *Quat. Sci. Rev.* **107**, 149–181 (2015).
74. Mangerud, J., Jansen, E. & Landvik, J. Y. Late Cenozoic history of the Scandinavian and Barents Sea ice sheets. *Glob. Planet. Change* **12**, 11–26 (1996).
75. Sutherland, R., Kim, K., Zondervan, A. & McSaveney, M. Orbital forcing of mid-latitude Southern Hemisphere glaciation since 100 ka inferred from cosmogenic nuclide ages of moraine boulders from the Cascade Plateau, southwest New Zealand. *Geo. Soc. Am. Bull.* **119**, 443–451 (2007).
76. Glasser, N. F. et al. Cosmogenic nuclide exposure ages for moraines in the Lago San Martin Valley, Argentina. *Quat. Res.* **75**, 636–646 (2011).
77. Briner, J. P. & Kaufman, D. S. Late Pleistocene mountain glaciation in Alaska: key chronologies. *J. Quat. Sci.* **23**, 659–670 (2008).
78. Phillips, L. Vegetational history of the Ipswichian/Eemian interglacial in Britain and continental Europe. *New Phytol.* **73**, 589–604 (1974).
79. Goelzer, H., Huybrechts, P., Loutre, M. F. & Fichefet, T. Last Interglacial climate and sea-level evolution from a coupled ice sheet–climate model. *Clim. Past.* **12**, 2195–2213 (2016).
80. McKay, N. P., Overpeck, J. T. & Otto-Bliesner, B. L. The role of ocean thermal expansion in Last Interglacial sea level rise. *Geophys. Res. Lett.* **38**, L14605 (2011).
81. Meehl, G. A. & Stocker, T. F. *Global Climate Projections* (Cambridge Univ. Press, New York, 2007).
82. Bauch, H. A. et al. Climatic bisection of the last interglacial warm period in the Polar North Atlantic. *Quat. Sci. Rev.* **30**, 1813–1818 (2011).
83. van de Plassche, O. *Sea-Level Research: A Manual for the Collection and Evaluation of Data* (GeoBooks, Norwich, 1986).
84. Rovere, A. et al. The analysis of Last Interglacial (MIS 5e) relative sea-level indicators: reconstructing sea-level in a warmer world. *Earth Sci. Rev.* **159**, 404–427 (2016).
85. Grant, K. et al. Rapid coupling between ice volume and polar temperature over the past 150,000 years. *Nature* **491**, 744–747 (2012).
86. Thompson, W. G., Curran, H. A., Wilson, M. A. & White, B. Sea-level oscillations during the last interglacial highstand recorded by Bahamas corals. *Nat. Geosci.* **4**, 684–687 (2011).
87. Dutton, A. et al. Tropical tales of polar ice: evidence of last interglacial polar ice sheet retreat recorded by fossil reefs of the granitic Seychelles islands. *Quat. Sci. Rev.* **107**, 182–196 (2015).
88. Hearty, P. J., Hollin, J. T., Neumann, A. C., O'Leary, M. J. & McCulloch, M. Global sea-level fluctuations during the Last Interglaciation (MIS 5e). *Quat. Sci. Rev.* **26**, 2090–2112 (2007).
89. White, B., Curran, H. A. & Wilson, M. A. Bahamian coral reefs yield evidence of a brief sea-level lowstand during the last interglacial. *Carbonate Evaporite* **13**, 10 (1998).
90. Hibbert, F. D. et al. Coral indicators of past sea-level change: a global repository of U-series dated benchmarks. *Quat. Sci. Rev.* **145**, 1–56 (2016).
91. Chen, J. H., Curran, H. A., White, B. & Wasserburg, G. J. Precise chronology of the last interglacial period: 234U-230Th data from fossil coral reefs in the Bahamas. *Geo. Soc. Am. Bull.* **103**, 82–97 (1991).
92. Muhs, D. R. & Simmons, K. R. Taphonomic problems in reconstructing sea-level history from the late Quaternary marine terraces of Barbados. *Quat. Res.* **88**, 409–429 (2017).
93. Stirling, C. H. & Andersen, M. B. Uranium-series dating of fossil coral reefs: extending the sea-level record beyond the last glacial cycle. *Earth Planet. Sci. Lett.* **284**, 269–283 (2009).
94. Milne, G. A. & Mitrovica, J. X. Searching for eustasy in deglacial sea-level histories. *Quat. Sci. Rev.* **27**, 2292–2302 (2008).
95. Vyverberg, K. et al. Episodic reef growth in the granitic Seychelles during the Last Interglacial: implications for polar ice sheet dynamics. *Mar. Geol.* **399**, 170–187 (2018).
96. Pan, T.-Y., Murray-Wallace, C. V., Dosseto, A. & Bourman, R. P. The last interglacial (MIS 5e) sea level highstand from a tectonically stable far-field setting, Yorke Peninsula, southern Australia. *Mar. Geol.* **398**, 126–136 (2018).
97. Blanchon, P., Eisenhauer, A., Fietzke, J. & Liebetrau, V. Rapid sea-level rise and reef back-stepping at the close of the last interglacial highstand. *Nature* **458**, 881–884 (2009).
98. Mauz, B., Shen, Z., Elmejdoub, N. & Spada, G. No evidence from the eastern Mediterranean for a MIS 5e double peak sea-level highstand. *Quat. Res.* **89**, 505–510 (2018).
99. Zagwijn, W. H. Sea-level changes in the Netherlands during the Eemian. *Geol. En. Mijnb.* **62**, 437–450 (1983).
100. Berger, A. & Loutre, M.-F. Insolation values for the climate of the last 10 million years. *Quat. Sci. Rev.* **10**, 297–317 (1991).
101. Schilt, A. et al. Atmospheric nitrous oxide during the last 140,000 years. *Earth Planet. Sci. Lett.* **300**, 33–43 (2010).

102. Petit, J.-R. et al. Climate and atmospheric history of the past 420,000 years from the Vostok ice core, Antarctica. *Nature* **399**, 429–436 (1999).
103. Barker, S. et al. Icebergs not the trigger for North Atlantic cold events. *Nature* **520**, 333–336 (2015).
104. Ho, S. L. et al. Sea surface temperature variability in the Pacific sector of the Southern Ocean over the past 700 kyr. *Paleoceanography* **27**, PA4202 (2012).
105. Cortese, G. & Abelmann, A. Radiolarian-based paleotemperatures during the last 160 kyr at ODP Site 1089 (Southern Ocean, Atlantic Sector). *Palaeogeogr. Palaeoclimatol. Palaeoecol.* **182**, 259–286 (2002).
106. Jouzel, J. et al. Orbital and millennial Antarctic climate variability over the past 800,000 years. *Science* **317**, 793–796 (2007).

Acknowledgements

N.L.M.B. and A.J.L. acknowledge funding from a UK Natural Environment Research Council (NERC) grant (NE/I008675/1). E.L.M. acknowledges funding support from a Philip Leverhulme Prize (2013). P.L.W. and S.S.R.J. acknowledge NERC Independent Research Fellowships (NE/K009958/1, NE/J018333/1). This paper has been the result of a several workshops funded by the Department of Geography at Durham University. The paper is a contribution to PALSEA (an INQUA International Focus Group and a PAGES working group), the INQUA Commission on Coastal and Marine Processes, the Sea Level and Coastal Change (SLaCC) working group and the Scientific Committee on Antarctic Research SERCE and PAIS programs.

Author contributions

N.L.M.B. and E.L.M. conceived and led the study. P.L.W. conducted the GIA modelling. All authors contributed ideas and to the development and writing of the paper.

Competing interests

The authors declare no competing interests.

Additional information

Supplementary information is available for this paper at https://doi.org/10.1038/s41561-018-0195-4.

Reprints and permissions information is available at www.nature.com/reprints.

Correspondence should be addressed to N.L.M.B.

Publisher's note: Springer Nature remains neutral with regard to jurisdictional claims in published maps and institutional affiliations.